

Electronic structure and Compton profile of CaH_2

This article has been downloaded from IOPscience. Please scroll down to see the full text article.

1994 J. Phys.: Condens. Matter 6 8539

(<http://iopscience.iop.org/0953-8984/6/41/016>)

View [the table of contents for this issue](#), or go to the [journal homepage](#) for more

Download details:

IP Address: 171.66.16.151

The article was downloaded on 12/05/2010 at 20:46

Please note that [terms and conditions apply](#).

Electronic structure and Compton profile of CaH_2

Chuan-Yun Xiao^{††}, Jin-Long Yang^{†§}, Kai-Ming Deng^{||}, Zu-He Bian[¶] and Ke-Lin Wang[§]

[†] China Center of Advanced Science and Technology (World Laboratory), PO Box 8730, Beijing 100080, People's Republic of China

^{††} Department of Physics, Central China Normal University, Wuhan, Hubei 430070, People's Republic of China

[§] Center for Fundamental Physics, University of Science and Technology of China, Hefei, Anhui 230026, People's Republic of China

^{||} Department of Applied Physics, East China Institute of Technology, Nanjing, Jiangsu 210014, People's Republic of China

[¶] Department of Modern Physics, University of Science and Technology of China, Hefei, Anhui 230026, People's Republic of China

Received 30 December 1993, in final form 10 May 1994

Abstract. First-principles studies are carried out on the electronic structure and Compton profile for the low-symmetry system of calcium dihydride using the discrete variational local-density-functional method with embedded cluster model. The results demonstrate that, with the ionic bonding picture, experimental data from photoelectron spectroscopy with both x-rays and synchrotron radiation and from Compton profile measurements can be reasonably understood. Based on the bonding character revealed in the electronic structure, we suggest that CaH_2 doped with a monovalent element could be a superconductor.

1. Introduction

Metal hydrides have received wide attention because of various technological applications and great scientific interest [1–3]. Hydrogen is believed to be the most promising energy carrier of the future, and metal hydrides are the most convenient carriers of hydrogen, among which the light-metal hydrides are considered to be the best candidates because of their high weight percentage of hydrogen [4]. In addition, interesting superconductivities have been found in some metal hydrides, of which a noted example is PdH_x , whose critical transition temperature was reported to increase sensitively with increasing concentration of hydrogen [5]. Metal hydrides are also important for the tests they provide of several theoretical models.

The bonding natures in metal hydrides are usually quite complex [6–8] and have been explored by various experimental and theoretical means. Historically, three simplified models [1, 9] have generally been employed to understand the experimental data from such diverse fields as photoelectron spectroscopy with x-rays (XPS) or synchrotron radiation (SRPES), measurements of Compton profile (CP), lattice energy, electronic specific heat and magnetic susceptibility [10, 11]. They are the anionic (I), the protonic (P) and the covalent (C) models (IPC models for short), corresponding to three types of extreme bonding in metal hydrides. The anionic model is based on the assumption that an electron from the metal ion is transferred to the hydrogen. The protonic model is in a sense the opposite of the anionic one; here the electron is assumed to leave the proton of the hydrogen and to join

the partially occupied metallic conduction band. In the covalent model, the hydrogen is assumed to bond covalently to the metal atoms. The purely anionic model was found to work well for the typically ionic alkali-metal hydrides. For some transition-metal hydrides such as TiH_x [11], the protonic model was found to be fairly successful. For some other systems such as NbH_x [12], however, different properties of the system cannot fit with a single model. As for the alkaline-earth-metal hydrides, BeH_2 is demonstrated to be purely covalent. MgH_2 was found to be intermediate between ionic and covalent from the study of lattice energy [13], but more recent band-structure calculations showed that MgH_2 is largely ionic with little covalency [14]. For CaH_2 , which is known as one of the three most useful light-metal hydrides (LiH , MgH_2 and CaH_2), although the ionic bonding picture was suggested from consideration of the well separated electronegativities of Ca and H, and was supported by the XPS study [8], the Compton profile measurement failed to be interpreted with either of the IPC models [7].

The failure of IPC models in these systems can be attributed to two main reasons. First, the solid-state bonding and structural effects are largely omitted in these models since they normally assumed a single 1s Slater-type orbital (1s STO) to describe the electron of the hydrogen and adopted the rigid-band approximation for the metal. However, Kunz [15] and Pattison *et al* [16] have shown that, because of the solid-state effects, the radial behaviour of the hydrogen wavefunction must differ appreciably from 1s STO. Secondly, these models have assumed extreme bonding character, while an appropriate mixed bonding picture among the IPC models would be more reasonable in the actual system.

The best way to understand completely the electronic properties of metal hydrides is proved to be by means of band-structure calculations. The pioneering work along this road was carried out by Switendick [17] in 1970 using an augmented plane-wave (APW) method, which showed the limits of the simplified descriptions in the IPC models, and several other band-structure methods have since been applied [14, 18, 19]. However, because of the low orthorhombic symmetry, no band-structure calculation has been available nor other first-principles studies reported for the CaH_2 system in its actual structure. Only a non-self-consistent APW band-structure calculation was performed by Weaver [20], where the complicated structure of CaH_2 was simplified to the hypothetical CaF_2 -type FCC structure. Since the structural effects are completely smeared out in this study, its results deserve to be re-examined by a calculation based on the actual structure. Moreover, the CP experiments of the system remain to be reasonably accounted for.

Related to the band-structure methods, but requiring much less computational effort, is the molecular approach utilizing a finite cluster of host atoms taken from the infinite solid to simulate the bulk properties. In this paper, first-principles calculations on both the electronic structure and the Compton profile of CaH_2 in the actual structure are performed by the discrete-variational local-density-functional (DV-LDF) method with cluster model. This method has proved to be very conducive to the study of systems with low symmetry for which the conventional band-structure approach proves intractable or computationally expensive [21]. Ellis *et al* [22] have successfully applied this method to study the photoelectron spectra and Compton profile of NbO_2 . Our model is based on the IPC models but we now take the structural and the bonding effects into consideration in a more reasonable way and hence our scheme is expected to be an improvement. In the following sections, we will describe the choice of our cluster model and relevant computational parameters in section 2, present our results and discussion in section 3 and summarize our conclusion in section 4.

2. Cluster model and computational parameters

The crystal structure and related parameters of CaH₂ are described by Wyckoff [23]. It is a complicated PbCl₂-type orthorhombic crystal with space group *Pnma* and with lattice constants $a = 6.838$, $b = 5.936$ and $c = 3.600$ Å. Each unit cell contains four CaH₂ molecules with two inequivalent hydrogen sites. All atoms in a unit cell are in the positions (in cell fraction) $\pm(u, v, 0.25)$ and $\pm(0.5-u, 0.5+v, 0.25)$ with the parameters $u = 0.010$ and $v = 0.240$ for Ca sites, $u = 0.430$ and $v = 0.240$ for H(1) sites, and $u = 0.742$ and $v = 0.004$ for H(2) sites. We choose the cluster CaH₁₁ consisting of Ca and its 11 nearest-neighbour hydrogens in our calculation to simulate bulk CaH₂, with Ca–H distance ranging from 1.884 to 2.995 Å. The coordinates of atoms in this cluster are listed in table 1. For the convenience of computation, our coordinate system (x, y, z) is slightly different from that of Wyckoff (a, b, c) with the mutual relationship $x = a$, $y = -c$ and $z = b$. This cluster has C_s symmetry with x and z axes in the mirror plane.

Table 1. Coordinates (au) of atoms in cluster CaH₁₁.

	Ca	H(1)	H(2)	H(3)	H(4)	H(5)
x	0.0	5.427 22	-3.463 08	-3.256 33	-1.033 76	-1.033 76
y	0.0	0.0	0.0	0.0	-3.401 51	3.401 51
z	0.0	0.0	-2.647 31	2.964 10	0.224 35	0.224 35
	H(6)	H(7)	H(8)	H(9)	H(10)	H(11)
x	2.997 89	2.997 89	3.204 64	3.204 64	0.775 32	0.775 32
y	-3.401 51	3.401 51	-3.401 51	3.401 51	0.0	0.0
z	2.871 66	2.871 66	-2.737 05	-2.737 05	5.608 71	-5.608 71

In principle, we should consider the cluster CaH₁₁ in three typical charge states, i.e. (CaH₁₁)⁹⁻, (CaH₁₁)⁹⁺ and (CaH₁₁)⁰, as assumed in corresponding IPC models to represent the three possible types of typical bonding in the system, and decide what charge-state model can provide a reasonable description of the electronic structure of CaH₂ by comparing the calculated results with experiments. However, since we know that both XPS [8] and SRPES [20] indicated that CaH₂ is a wide-band-gap insulator with a gap of 5 eV, and that Ca has two 4s electrons with well separated electronegativity (1.0) from H (2.2), a charge transfer from Ca to H would lead to an ionic bonding picture, so we can start directly with the anionic model (CaH₁₁)⁹⁻. This choice will be tested by its agreement with experiments, to see how reasonable it is. The influence of the rest of the solid on the cluster is considered with the embedded cluster scheme, in which the cluster is embedded in a microcrystal extending out to 17–20 au from the centre of the cluster and consisting of hundreds of atoms (236 atoms here) to simulate the rest of the solid, and the charge density that generates both the Coulomb and the exchange–correlation potentials now includes the contributions both from the cluster and from the embedding lattice [24].

The DV-LDF method is used to obtain the one-electron wavefunction and associated eigenvalues of our cluster. This method is a kind of molecular-orbital calculation approach within the LDF formalism and has been described in detail elsewhere [25–27]. Here we only point out some key features relevant to our purpose. In the method, the molecular orbitals are constructed by symmetry-adapted atomic orbitals with the linear combination of atomic orbitals (LCAO) scheme, and the secular equation is solved iteratively. The bonding character of each molecular orbital can be analysed from the Mulliken populations. Since the initial charge states attached to Ca and H in our method will adjust during the iteration

to reach self-consistency, this scheme can reflect to some extent the possible mixture of different bonding characters in the system. The Hamiltonian and the overlap matrices in the secular equation are evaluated as weighted sums over a set of Diophantine sampling points, thereby avoiding quantities of multicentred integrals and reducing the computer space and time.

In our calculations, the spin-restricted scheme is adopted. The exchange–correlation potential is taken to be of the von Barth–Hedin form [28] with parameter taken from Moruzzi *et al* [29]. The variational basis set is chosen to be the numerical atomic single-site orbitals, i.e. 1s–4p of Ca and 1s–2s of H atoms, each compacted by a funnel potential well [30] of depth 5.0 au extending from 2.0 to 4.0 au. A total number of 3600 sampling points is used in the numerical integration scheme. The convergence accuracy of our self-consistent-charge process (SCC approximation) is $10^{-4} e$.

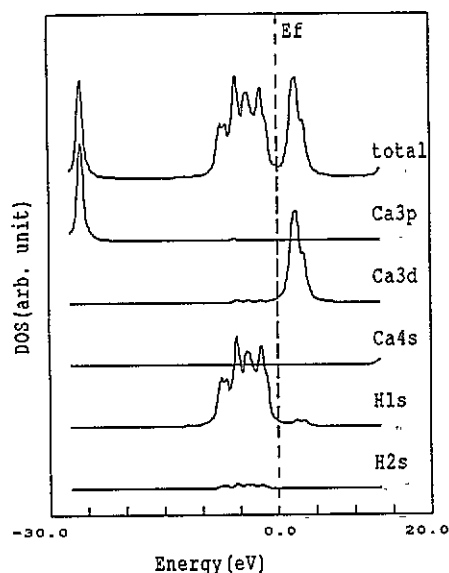


Figure 1. Total and partial densities of states for the cluster model.

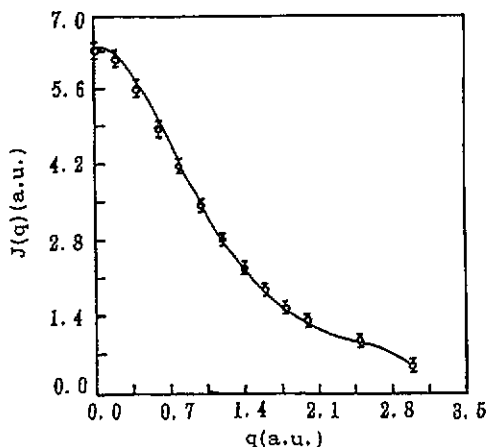


Figure 2. Schematic comparison of the calculated Compton profile for the cluster model (—) with the experimental profile (O) of CaH_2 .

3. Results and discussion

3.1. Electronic structure

Figure 1 shows the total and partial densities of states (TDOS and PDOS) for our cluster model, which are obtained by a Gaussian extension [26] of the ground-state one-electron energy levels to simulate the solid-state band structure and can be compared with the measured XPS [8] or SRPES [20]. From this figure, we see that the Fermi level (E_f) lies at the valley of the DOS above the filled valence band and there is a gap of about 3.32 eV between the HOMO (highest occupied molecular orbital) and the LUMO (lowest unoccupied molecular orbital). Considering that LDF theory usually underestimates the band gap of semiconductors and

insulators by about 40% [14], this result indicates that CaH_2 should be an insulator with a band gap of about 5 eV. Our expectation is in good agreement with the XPS and the SRPES measurements [8, 20], both of which indicated that CaH_2 is an insulator whose electronic states do not exist within about 2.5 eV of E_f , demonstrating that our choice of anionic model is reasonable to describe CaH_2 .

Table 2. Comparison of the calculated electronic structure for the cluster model with the experimental data of CaH_2 (eV). VBW stands for the valence bandwidth and E_g for the gap. The distances from E_f to the centres of several bands are also presented.

	E_g	VBW	E_f to VB centre	E_f to Ca 3p band	E_f to Ca 3s band
Calc.	3.321	5.994	4.658	25.847	44.122
Exp.	5.0 [20]	6.0 [20]	5.0 [20]	~26.0 [20]	—

Further, we see that our calculated electronic structure consists of the following three parts (relative to E_f): levels between -25.7 and -26.0 eV are Ca 3p non-bonding orbitals, corresponding to the Ca 3p core band; levels between -1.66 and -7.65 eV are the bonding orbitals consisting of the hybrids of H 1s, H 2s and Ca 3d orbitals; and levels above E_f are, successively, Ca 3d-, Ca 4s-, Ca 4p- and H 2s-dominated antibonding orbitals. It is worth noticing that the Ca-related levels are in the order Ca 3d, Ca 4s, Ca 4p rather than in the order of Ca 4s, Ca 4p, Ca 3d, so we find little Ca 4s and Ca 4p states below E_f . This order of levels is different from the order in an isolated neutral Ca atom (4s, 4p, 3d) but is the same as that in ionic Ca^{2+} , supporting our ionic bonding picture. Table 2 lists some data of the electronic structure for our model. Their good agreement with the available experimental data quantitatively supports the anionic model. The bonding character of each band can be observed by the Mulliken population analysis [31] of the molecular orbitals, as revealed by the PDOS in figure 1. The valence band is predominantly of H 1s character, mixed slightly with Ca 3d ($\sim 5\%$) and H 2s ($\sim 7\%$). The fact that the valence band is rather broad, unlike that of an isolated H^- ion, implies that the interaction between H^- ions in CaH_2 should be rather strong. The empty Ca 3d band is also essentially pure, mixed with H 1s by no more than 8%. These bonding features show that CaH_2 is a strongly ionic solid with weak covalency. This conclusion can also be seen from the effective charge for Ca and H obtained from the Mulliken analysis. Although the Mulliken population has some uncertainty, we believe its value is at least qualitatively reasonable. Besides, since Ca locates at the centre of the cluster while hydrogens lie outside and have very different stoichiometry from the bulk, only the effective charge for Ca can be reliable. We obtained the effective charges for Ca to be $1.61e$, which is close to the estimate of $1.3e$ from the XPS study [8]. A similar conclusion has been drawn for MgH_2 by Yu and Lam in an *ab initio* pseudopotential band calculation [14], where no covalent bonding was found. However, our conclusion is noticeably different from Weaver's model calculation [20], where considerable Ca d and Ca p characters appeared in the hybrid states of the bonding band, indicating the importance of covalency.

Based on the above results, let us now discuss an interesting problem. It is worth noticing that the electronic structure and the associated bonding character we obtained for CaH_2 are similar to those obtained by Yu and Lam for MgH_2 (see figures 4 and 6 in [14]). Both systems are strongly ionic solids with similar experimental band gap of about 5 eV, and have a valence band predominated by hydrogen orbitals. Moreover, their DOS at E_f are both very high. Based on these features revealed in their electronic structure, and applying

the rigid-band model, which is valid to the first-order approximation, Yu and Lam inferred that MgH_2 doped with a monovalent element could be a superconductor. Their inference was made from three observations, which in our case can be stated as follows:

(i) According to the nature of electronic structure of CaH_2 and the rigid-band approximation, CaH_2 can be made metallic if it is doped substitutionally with a monovalent element.

(ii) The carriers of the doped CaH_2 system will be of the hole type whose orbitals will be mainly of H character.

(iii) The DOS for the doped CaH_2 will be very high.

With the above observations, one may, just as Yu and Lam did for doped MgH_2 , think of doped CaH_2 as a metallic-hydrogen system that is stabilized by Ca and is made metallic via doping. Then this system could be a high-temperature superconductor for the same reasons as metallic hydrogen could be. Overhauser [32] has also suggested this idea for LiBeH_3 and LiBeH_4 after an analysis of their structures. Since Na^+ has a similar radius to Ca^{2+} , we suggest that Na could be a candidate as the dopant. By the way, the dopant level is difficult to predict; Yu and Lam estimated it to be 10–20% for MgH_2 by a comparison with the oxide superconductors. In contrast to metallic hydrogen, whose valence band is half-filled, the valence band of the doped CaH_2 system is mostly filled since the carriers in this system are the holes whose concentration depends on the doping level. Yu and Lam also suggested annealing the sample under hydrogen atmosphere so as to reduce hydrogen vacancies resulting from charge compensation in the ionic system. Further evidence is expected to confirm the suggestions presented here.

3.2. Compton profile

Compton scattering has become a powerful way of investigating the electronic structure of hydrides in recent years [7]. The CP is related to the momentum density of the material's ground state and has been demonstrated to be rather sensitive to the bonding nature in several other metal hydrides [10, 11, 33]. The comparison of the theoretical with the experimental profiles can therefore act as a probe to test the validity of different theoretical models.

In the non-relativistic limit and the impulse approximation, the isotropic Compton profile for a polycrystalline system is given by [22, 34]:

$$J(q) = 2\pi \int_q^\infty p \langle \rho(p) \rangle dp \quad (1)$$

where $\langle \rho(p) \rangle$ is the spherical average of the crystal momentum density defined as

$$\rho(p) = \sum_i f_i |\phi_i(p)|^2 \quad (2)$$

where f_i is the occupation number of the i th molecular orbital of the system and $\phi_i(p)$ is the momentum-space wavefunction obtained by Fourier-transforming the real-space wavefunction $\psi_i(r)$:

$$\phi_i(p) = \frac{1}{(2\pi)^{3/2}} \int \psi_i(r) \exp(-ip \cdot r) d^3r. \quad (3)$$

The CP is thus obtainable from $\psi_i(r)$ through equations (1–3).

Before this scheme is applied to calculate the CP of CaH_2 crystal with the cluster model, it should be noted that the momentum density of the CaH_2 crystal cannot be replaced directly by that of the CaH_{11} cluster, since they do not have the same stoichiometry. We correlate them by the following scaling procedure [22]. The cluster momentum density is a sum over occupied molecular orbitals and the molecular orbitals are linear combinations of atomic orbitals (LCAO scheme). Hence the cluster momentum density can be decomposed into (Ca–Ca), (H–H) and (Ca–H) terms. The CaH_2 crystal momentum density can thus be obtained from that of the CaH_{11} cluster by scaling the (H–H) and (Ca–H) terms by 2/11 and 1/4, respectively.

With the above scheme, the CP of CaH_2 is calculated with our cluster model. Experimentally, study on CaH_2 was made by measuring the difference CP $\Delta J(q)$ of CaH_2 and metallic Ca, which is defined as the CP $J_{\text{CaH}_2}(q)$ of CaH_2 minus the CP $J_{\text{Ca}}(q)$ of Ca, so as to simplify the interpretation of the effect of hydrogen on the hydride and meanwhile minimize various systematic errors [7]. Since no experimental data for CaH_2 are directly available, we take the sum of $\Delta J^{\text{exp}}(q)$ in [7] and $J_{\text{Ca}}^{\text{exp}}(q)$ in [35] as the experimental value $J_{\text{CaH}_2}^{\text{exp}}(q)$ with which to compare our calculated results $J_{\text{CaH}_2}^{\text{calc}}(q)$, where $J_{\text{Ca}}^{\text{exp}}(q)$ and $J_{\text{CaH}_2}^{\text{calc}}(q)$ have been convoluted with the instrumental resolution function of full width at half-maximum (FWHM) 0.6 au in [7] because the $\Delta J^{\text{exp}}(q)$ were non-deconvoluted. It is to avoid the uncertainty inherent in the deconvolution process, especially for such small quantities as $\Delta J^{\text{exp}}(q)$, that we choose to take the convolute of both $J_{\text{Ca}}^{\text{exp}}(q)$ and $J_{\text{CaH}_2}^{\text{calc}}(q)$ instead of taking the deconvolute of only $\Delta J^{\text{exp}}(q)$. Such a sum procedure may of course bring about some extra errors, so further Compton profile measurement directly for CaH_2 is expected for better comparison. The theoretical and experimental CP thus obtained are given in table 3 and shown in figure 2. For comparison, we also list the sum of free-ion Compton profiles for one Ca^{2+} and two H^- in table 3. Each profile is normalized to 16.694 electrons from -3 to $+3$ au in momentum space. Our calculated profile for the anionic model is found to reproduce the experimental values fairly well within the considerably large experimental error bars. We also find that the cluster model profile is rather close to the summed free-ion profile: both profiles are nearly the same in the high-momentum region, while the former is smaller by about 5% in the low-momentum region and higher by 4% in the intermediate-momentum region. Since the CP in the low-momentum region is contributed by the valence electrons and the valence band of CaH_2 is dominantly of H character, this difference can be attributed to the interaction between H^- ions in bulk CaH_2 and means that the valence electrons are more bound in the system than in the free ions. Recalling that the anionic model with simpler 1s STO cannot fit with the experimental CP, our result, which arises from the combination of the cluster model and the scaling procedure, indicates the importance of the correct wavefunction to reflect the structural and solid effects. From the above discussions, we can say that our calculations on both the electronic structure and the CP consistently demonstrate the reasonableness of the anionic model to describe CaH_2 .

4. Conclusion

In this paper, we have performed first-principles calculations for CaH_2 in its actual low-symmetry structure within the local-density-functional formalism. With the embedded cluster model, we have discussed the bonding character in CaH_2 , and it is found that the anionic model can provide quantitatively reasonable descriptions for both the electronic structure and the Compton profile of the system. The results are compatible with the well

Table 3. The calculated and measured Compton profiles for CaH_2 together with the free-ion profile. The profiles are convoluted with the resolution function of $\text{FWHM} = 0.6$ au and normalized to 16,694 electrons from -3.0 to $+3.0$ au.

$J(q)$				$J(q)$			
q	Cluster	$\text{Ca}^{2+} + 2\text{H}^-$	Exp	q	Cluster	$\text{Ca}^{2+} + 2\text{H}^-$	Exp
0.0	6.399	6.685	6.340 ± 0.2	1.6	1.854	1.802	1.927 ± 0.1
0.1	6.356	6.599		1.7	1.681	1.636	
0.2	6.225	6.423	6.17 ± 0.2	1.8	1.531	1.492	1.598 ± 0.1
0.3	6.016	6.169		1.9	1.402	1.368	
0.4	5.740	5.849	5.625 ± 0.2	2.0	1.291	1.261	1.358 ± 0.1
0.5	5.410	5.478		2.1	1.196	1.169	
0.6	5.042	5.072	4.877 ± 0.2	2.2	1.114	1.023	
0.7	4.654	4.652		2.3	1.044	1.023	
0.8	4.260	4.231	4.191 ± 0.2	2.4	0.984	0.965	
0.9	3.870	3.818		2.5	0.930	0.913	0.986 ± 0.1
1.0	3.498	3.429	3.452 ± 0.1	2.6	0.877	0.862	
1.1	3.149	3.066		2.7	0.817	0.804	
1.2	2.828	2.736	2.852 ± 0.1	2.8	0.739	0.728	
1.3	2.538	2.439		2.9	0.633	0.624	
1.4	2.280	2.176	2.325 ± 0.1	3.0	0.501	0.494	0.540 ± 0.1
1.5	2.053	1.993					

separated electronegativities of Ca and H, and are in fair agreement with the XPS, the SRPES and the Compton profile experiments. The results of the electronic structure show that CaH_2 is a strongly ionic solid with weak covalency, and that the valence band is predominantly of H character with slight admixture of Ca orbitals. Based on our results of the electronic structure and following a similar discussion of Yu and Lam, we suggest that CaH_2 substitutionally doped with a monovalent element such as Na could become a high-temperature superconductor.

Acknowledgments

We are grateful to Dr Wei Liu, Open Laboratory of Internal Friction and Defects in Solids, University of Science and Technology of China, for his helpful discussions concerning superconductivity. This project is supported partly by the National Natural Science Foundation of China and partly by the Natural Science Foundation of Central China Normal University.

References

- [1] Libowitz G G 1965 *Solid-State Chemistry of Binary Metal Hydrides* (New York: Benjamin)
- [2] Reilly J J and Sandrock G D 1980 *Sci. Am.* **242** 98
- [3] Jean P and Satterthwaite C H (ed) 1983 *Electronic Structure and Properties of Hydrogen in Metals* (New York: Plenum)
- [4] Reilly J J 1978 *Proc. Int. Symp. on Hydrides for Energy Storage (Geilo, Norway, 1977)* ed A F Anderson and A J Maelland (Oxford: Pergamon)
- [5] Skiskiewicz T 1972 *Phys. Status Solidi A* **11** K123
- [6] Felsteiner J, Heilper M, Gertner I, Tanner A C, Opher R and Berggren K F 1981 *Phys. Rev. B* **23** 5156
- [7] Alexandropoulos N G, Chatzigeorgiou T and Theodoridou I 1988 *Phil. Mag. B* **57** 191

- [8] Franzen H F, Merrick J, Urmana M, Khan A S, Peterson D T, McCreary J R and Thorn R J 1977 *J. Electron. Spectrosc. Relat. Phenom.* **11** 439
- [9] Fast J D 1976 *Cases in Metals* (London: Macmillan)
- [10] Lasser R and Lengeler B 1978 *Phys. Rev. B* **18** 637
- [11] Alexandropoulos N G, Theororidou I and Cooper M J 1987 *J. Phys. C: Solid State Phys.* **20** 1201
- [12] Theororidou I and Alexandropoulos N G 1984 *Z. Phys. B* **54** 22
- [13] Stander C M and Paaacey A 1978 *J. Phys. Chem. Solids* **39** 829
- [14] Yu J R and Lam P K 1988 *Phys. Rev. B* **37** 8730
- [15] Kunz A B 1969 *Phys. Status Solidi* **36** 301
- [16] Pattison P and Weyrich W 1979 *J. Phys. Chem. Solids* **40** 213
- [17] Switendick A C 1970 *Solid State Commun.* **8** 1463
- [18] Peterman D J, Harmon B N and Marchiando J 1979 *Phys. Rev. B* **19** 4867
- [19] Ameri S 1981 *Phys. Rev. B* **23** 4242
- [20] Weaver J H, Gupta M and Peterson D T 1984 *Solid State Commun.* **51** 805
- [21] Press M R and Ellis D E 1987 *Phys. Rev. B* **35** 4438
- [22] Umrigar C and Ellis D E 1980 *Phys. Rev. B* **21** 852
- [23] Wyckoff R W G 1963 *Crystal Structure* vol 1 (New York: Wiley)
- [24] Ellis D E, Benesh G A and Byrom E 1979 *Phys. Rev. B* **20** 1198
- [25] Rosen A, Ellis D E, Adachi H and Averil F W 1976 *J. Chem. Phys.* **65** 3629
- [26] Lindgren B and Ellis D E 1982 *Phys. Rev. B* **26** 636
- [27] Yang Jinlong, Xiao Chuanyun, Xia Shangda and Wang Kelin 1992 *Phys. Rev. B* **46** 13 709
- [28] von Barth U and Hedin L 1972 *J. Phys. C: Solid State Phys.* **5** 1629
- [29] Moruzzi V L, Janak J F and Williams A R 1978 *Calculated Electronic Properties of Metals* (New York: Pergamon)
- [30] Xia Shangda, Guo Changxin, Lin Libin and Ellis D E 1987 *Phys. Rev. B* **35** 7671
- [31] Mulliken R S 1955 *J. Chem. Phys.* **23** 411
- [32] Overhauser A W 1987 *Phys. Rev. B* **35** 411
- [33] Garreau Y and Louypias G 1990 *Solid State Commun.* **74** 583
- [34] Huibin Lan, Jinglong Yang and Kelin Wang 1990 *Phys. Lett.* **144A** 419
- [35] Aikala O 1975 *Phil. Mag.* **31** 935